1874-1495/20 *Send Orders for Reprints to reprints@benthamscience.net*

The Open Civil Engineering Journal

Content list available at: https://opencivilengineeringjournal.com

RESEARCH ARTICLE

Morphological and Physical Characteristic of Stone Mastic Asphalt Mixture Incorporating Nano Silica

Khairil A. Masri[1,2], Ramadhansyah Putra Jaya[1,*], Ahmad K. Arshad[3] and Mohd Zul H. Mahmud[4]

[1]*Department of Civil Engineering, College of Engineering, Universiti Malaysia Pahang, 26300 Gambang, Pahang, Malaysia*
[2]*Earth Resources and Sustainability Centre (ERAS), Universiti Malaysia Pahang, 26300 Gambang, Pahang, Malaysia*
[3]*Institute for Infrastructure Engineering and Sustainable Management (IIESM), Universiti Teknologi MARA, 40450 Shah Alam, Selangor, Malaysia*
[4]*School of Civil Engineering, Faculty of Engineering, Universiti Teknologi Malaysia, 81310, Johor Bahru, Malaysia*

Abstract:

Introduction:

Asphalt binder plays an important role in contributing to the good performance of asphalt mixture. However, the interlocking structure of asphalt binder is delicate and sensitive due to surrounding temperature and moisture.

Methods:

Previously, asphalt binder usually modified with polymer modifier. But, this type of modifier has low temperature susceptibility. To overcome this, nanomaterial is introduced to enhance the performance of virgin asphalt binder. Among the crucial evaluation of nano-modification is to evaluate its microstructural changes through morphological property evaluation. The addition of nanomaterial then will significantly improve the inner structure of asphalt binder and reduce the effect of those problems.

Aim:

Thus, the aim of this study was to assess the morphological properties of nanosilica modified asphalt binder to determine the inner structured properties of modified specimen.

Results:

Among the morphological tests conducted for asphalt binder in this study were Scanning Electron Microscope (SEM), X-Ray Diffraction (XRD) and Atomic Force Microscope (AFM). From SEM image analysis and XRD evaluation, the existence of Nanosilica (NS) inside the asphalt binder was well dispersed and from these two tests, the existence of NS inside asphalt binder was verified. From AFM results, most of NS-MB images before and after ageing conditions displayed the typical bee structure (Catana Phase).

Conclusion:

It was also concluded that the addition of NS in asphalt binder improved its surface stiffness. The overall surface stiffness of the asphalt binder after aging was increased and the surface became more solid.

Keywords: Morphological, Physical, Nano silica, Bitumen, Stone mastic asphalt, Catana phase.

Article History	Received: January 06, 2020	Revised: March 18, 2020	Accepted: April 15, 2020

1. INTRODUCTION

Nowadays, asphalt is mainly used as a binder for mineral aggregates in the paving industry. It is a complex hydrocarbon with composition are divided into four main components, lighter components such as aromatics and saturates and heavier components, asphaltenes and resins [1]. Although only a small amount of asphalt binder is used in a typical asphalt mixture, it plays an integral role in the performance of asphalt mixtures [2]. When the asphaltic materials do not satisfy the requirements for constructing a well-performing bituminous structure, modification usually is adopted as one of the best and most attractive strategies for meeting the desired properties of used materials [3]. It has been confirmed that asphalt aging is

* Address correspondence to this author at the Department of Civil Engineering, College of Engineering, Universiti Malaysia Pahang, 26300 Gambang, Pahang, Malaysia; E-mail:ramadhansyah@ump.edu.my

one of the most severe threats to the durability performance of asphalt pavement, and the aged asphalt material can be easily cracked by the traffic impact loading [4]. The aged asphalt pavement would also become brittle and have weak resistance to fatigue cracking [5]. Among the potential modifier that may increase the properties of asphalt binder is nanosilica [6]. Due to the number of factors affecting the behavior of conventional asphalt binders, a more advanced characterization is necessary to study the behavior of this material [7]. During the last few years the ability to evaluate asphalt binder using an AFM has resulted in considerable enhancements in the understanding of the asphalt binder microstructure and behaviour. Techniques for using the AFM to investigate the asphalt binder microstructure have also significantly improved during this time. Pizzorno *et al*. [8] were among the first researchers to report the existence of the so-called 'bee' structures with an oblong-shaped outline and rippled topography. They reported an increment in these bee structures with the increment in asphaltene content. Some researchers also reported that for some AFM devices, the laser used during the imaging process seemed to dissolve the bee structures. Subsequent work by Pauli *et al.* [9] demonstrated that the formation of such structures was attributed to the presence of waxes in asphalt binders. A more recent study by Allen *et al*. [10] also examined these bee structures. They reported an increment in the formation of bee structures with the ageing of the asphalt binder. They were able to use AFM indentation to measure viscoelastic creep properties for the different identifiable phases within the asphalt binder [11, 12]. In order to characterize the nano-structure, micro-structure and the mechanical behavior of asphalt binder, X-ray diffraction (XRD) experiments are conducted on asphalt binders modified with different contents. The XRD results usually indicated whether the composite exfoliated structure is within the nano-composite. In addition, the XRD images also show the interaction between nano layers and distinct asphalt binder domains containing "bee-like" structures as compared to the flat asphalt binder matrix [13]. Besides that, XRD Test can also determine the mineralogical compositions of material [14]. In addition, XRD is useful to measure d-spacing of ordered intercalated material [15]. Thus, this study is important to evaluate the effect of nanosilica towards the inner structure improvement of nanosilica modified asphalt binder. The most innovative contribution of this paper is related to the comprehensive assessment of the changes observed in the inner structure of asphalt binder that will significantly improve the overall performance of flexible pavement. A fundamental reason why the conventional asphalt binder greatly suffers from the ageing process will be revealed. This will provide the guidance and reference for industry to construct better and more durable pavement in the future.

2. MATERIALS AND METHODS

2.1. Asphalt Binder

Asphalt binder that was used in this study was penetration 60-70 modified with 0-5% nanosilica at increments of 1%. Table **1** summarizes the physical properties of asphalt binder [16].

2.2. Nanosilica

Nanosilica that was used in this study was in colloidal form. Table **2** shows the properties of Nanosilica [16].

2.3. Ageing Condition

The asphalt binder specimens were prepared in three different conditions which were unaged, short-term aged and long-term aged. Rolling Thin Film Oven (RTFO) equipment was used to simulate short term aging according to ASTM D2872 [17]. The RTFO also allows the determination of the mass of volatile that lost during the aging process of binders. In this test, the hot binder was poured into cylindrical glass bottles weighing 35 g each. The glass bottles containing the binder were placed horizontally in rotating carriage slots in the oven. Then, the carriage was rotated at a rate of 15 rpm for 75 minutes in the oven at temperature of 163°C. Throughout the test, the open glass bottles containing the binders were exposed to the air pressure at 4000 ml/min. Then, the Pressure Ageing Vessel (PAV) equipment was used to simulate long-term ageing of asphalt binder after 5 to 10 years. The binder was exposed to high pressure and temperature for 20 hours to simulate the effect of long-term oxidative ageing.

Table 1. Physical properties of asphalt binder.

Test	Nanosilica (%)					
	0	**1**	**2**	**3**	**4**	**5**
Softening Point	52.3	58.9	60.3	62.4	63.4	60.0
Penetration	65.0	43.5	41.1	33.3	29.1	30.7
Penetration Index	+0.1	+0.4	+0.8	+0.6	+0.5	0
Ductility	140.0	129.0	85.5	70.2	51.7	46.3
Storage Stability	0	0.2	0.2	0.2	0.3	0.5

Table 2. Properties of nanosilica

Properties	Value
Appearance	Slight Milky Transparent
SiO_2 (%)	30%
Na_2O (%)	0.5%
pH	8.5-10.5
Density	1.19-1.22 g/cm3
Particle Size	10-15 m

2.3.1. Morphological Properties

2.3.1.1. Scanning Electron Microscope

In order to observe the characteristics and structures of micro- and nanomaterials, the SEM (SU 7000) tests were conducted for 0% NS-MB (PEN 60-70) and 1 to 5% NS-MB (6 samples). The SEM permits ultra-high resolution imaging of thin films and semi-conductor materials on clean specimens [18]. The SEM permits ultra-high resolution imaging of thin films and semi-conductor materials on clean specimens [19]. The binder samples were flash frozen using liquid nitrogen and then placed in the SEM chamber at -26°C under a pressure of 30 Pa. the cryogenic stage was used to reduce changes in the binder structure due to heating by 20 kV electron beam.

2.3.1.2. X-Ray Diffraction

The XRD (X8 Apex) was used to provide a quantitative analysis of the interlayer gallery spacing and it provides a way to determine the extent of dispersion of the nanosilica in the PEN 60-70 asphalt binder. In the XRD technique, Bragg's law of diffraction was used to measure d-spacing between the nanosilica particles. Spacing change (increase or decrease) information can be used to determine the type of dispersion. For example, no d-spacing change indicates immiscible, increase in d-spacing indicates intercalated, and no distinct peak in the signal indicates exfoliation. In the case of peak in the signal, the d-spacing can be determined as shown in equation **1**.

$$d = \lambda/2\sin\Theta \quad \textbf{(1)}$$

Where;

λ = Wavelength of X-ray Source (λ=1.54 angstrom)

θ = Diffraction Angle

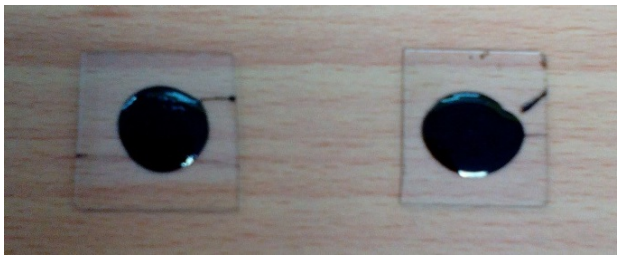

Fig. (1). AFM Specimens.

2.3.1.3. Atomic Force Microscopy

AFM was applied to investigate the morphology and microstructure of asphalt binder with the addition of NS. The specimens were divided into three different types which were unaged NS-MB, short-term aged NS-MB and long-term aged NS-MB. In the AFM sample preparation, NSMB was heated up to 160°C and dropped on glass slide surface. Glass slide was placed in oven at same temperature for 10 minutes in order to have a smooth and glossy surface. The samples were cooled at room temperature for 24 hours before tested. The dimension of asphalt droplet should be around 1 cm in diameter as shown in Fig. (**1**). Furthermore, the sample must keep in a closed container to prevent the sample surface from any disturbance such as dust. This is because the disturbed sample surface will highly affect the AFM image [20 - 22]. In this study, non-contact AFM (model EX-100) was used. The topographic image was scanned using a silicon probe. The cantilever was 125 µm long with a curvature radius of 5-10 µm. The drive frequency was about 300 kHz and the scan rate was 0.5 Hz. All AFM images were measured in a dimension of 20 µm x 20 µm.

2.3.1.4. Marshall Properties

Marshall Equipment was used to determine the volumetric properties of asphalt mixture. Among the parameters obtained from this test are stability, flow and density. To perform this test, three compacted asphalt mixture specimens were prepared for each binder content. Then, those specimens were placed transversely to the load actuator. The load was applied until the specimen broke. Finally, the value of stability and flow were recorded. This test was conducted in accordance with Malaysian Specification for Road Works [23].

3. RESULTS AND DISCUSSION

3.1. Scanning Electron Microscope

In order to understand the microstructure changes of NS-MB and the physical dispersion of the nanosilica particles in asphalt binder, Scanning Electron Microscopy (SEM) was used. Fig. (**2**) shows the SEM image of 0% to 5% NS-MB. It could be seen that microstructure of NS-MB changed significantly compared to control asphalt binder. The white spots shown in SEM image especially at 4% NS-MB represent nanosilica particles, thus the SEM image of modified asphalt binder shows well-dispersed nanosilica particles in the asphalt matrix. Thus, a new structure of asphalt binder was developed. However, nanosilica seemed to agglomerate in asphalt binder whereby the nanosilica become tens or hundreds nanometer in size. Due to the agglomeration of nanosilica, the surface area and reaction between nanosilica and asphalt binder become smaller. Therefore, the performance enhancement of asphalt binder with the addition of NS could not be fully achieved due to this agglomeration problem. Thus, well dispersion of nanosilica in asphalt binder may be helpful for the modulus improvement of nanosilica modified asphalt binder and mixture.

3.2. X-Ray Diffraction

Figs. (**3** and **4**) Show the X-ray diffraction results and d-spacing value for various amounts of NS-MB. From Fig. (**3**), unmodified specimen produced an amorphous line while modified specimen produced a semi crystalline structure. Theoretically, the asphalt binder is a typical amorphous material, thus the existence of nanosilica inside the binder increases the interlayer spacing, producing a main peak. This main peak produces a semi crystalline structure of NS-MB. Thus, it can prove the existence of NS inside the asphalt binder and the asphalt binder was able to intercalate with nanosilica. Fig. (**4**) shows the value of d-spacing for all NS-MB with mean value of 4.7. D-spacing is important in determining the dispersion level of NS inside asphalt binder based on Bragg's Law. From the result, it could be seen that the various amount of NS dispersed well inside the asphalt binder. D-spacing value is increased from 0 to maximum of 4.79 with the existence of NS. From 1% NS-MB to 3% NS-MB, the increment is about 2% while it continuously dropped at more than 3% NS-MB. This shows that NS densified the inner structure of the virgin asphalt binder [24, 25].

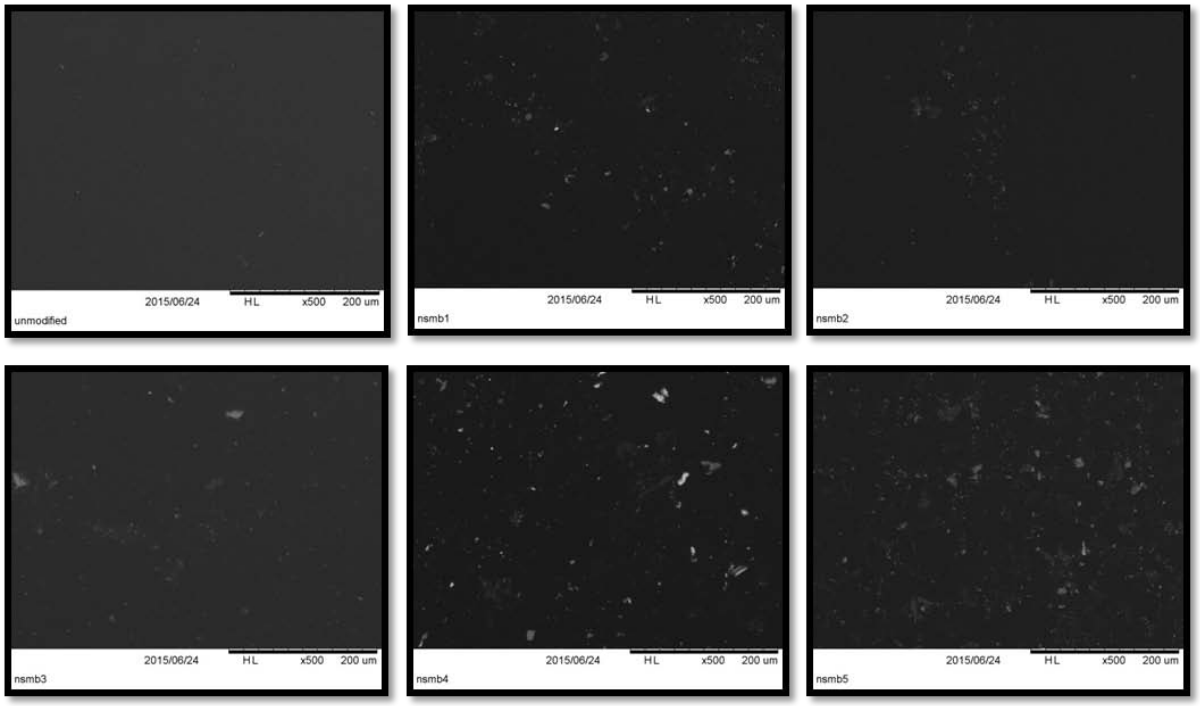

Fig (2). SEM Images for NS-MB.

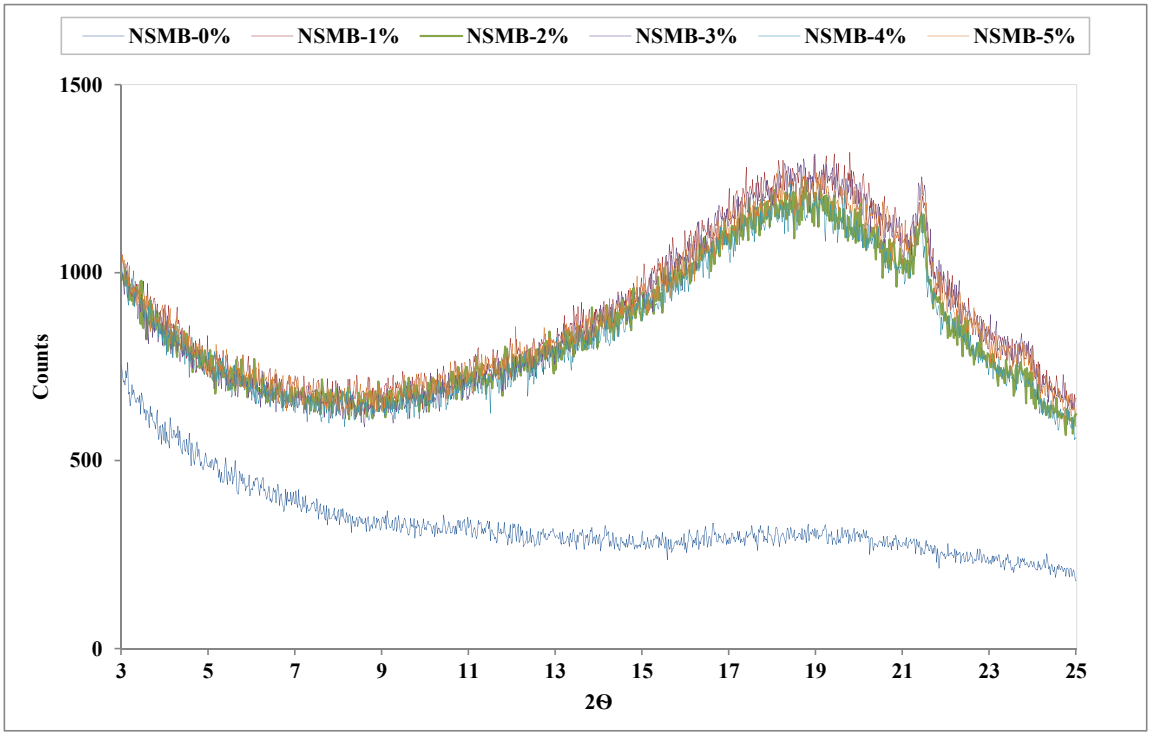

Fig (3). XRD for NS-MB.

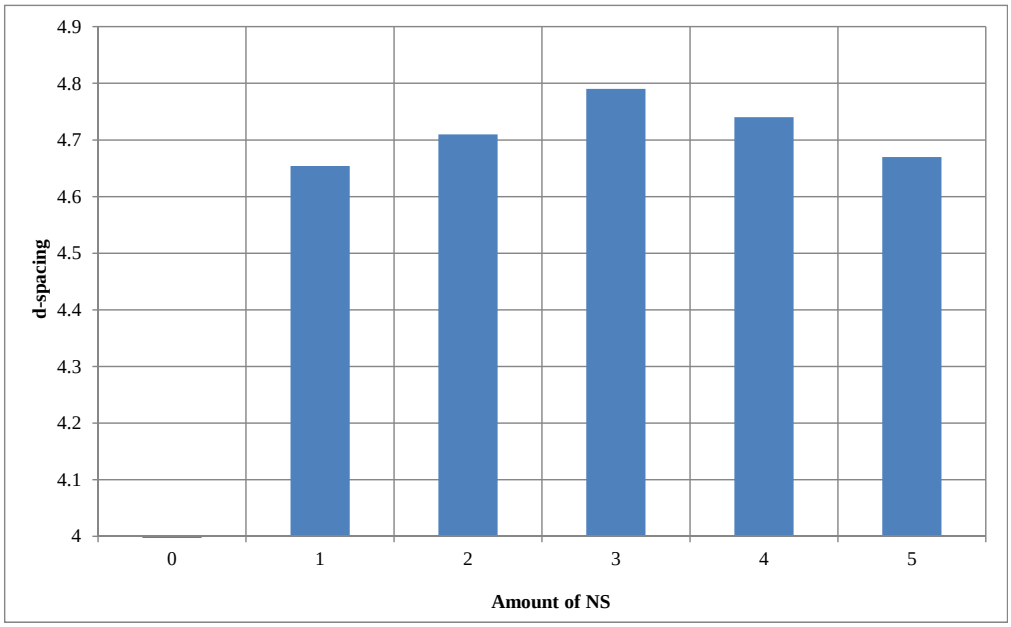

Fig (4). D-spacing Value for NS-MB.

3.3. Atomic Force Microscopy

3.3.1. Unaged NS-MB

Figs. (**5** and **6**) show the AFM topography image of unaged NS-MB samples. From the images shown, three distinctive phases were clearly identified for both control and modified binder. The addition of 1% and 2% NS significantly affected the AFM image where the amount of catana phase was increased by about 30% and 50% respectively. Meanwhile, for 3%, 4% and 5% NS-MB, those images only displayed almost the same graphic as control sample (0% NS-MB). The overall size of catana phase was nearly the same for all samples which were approximately 7 µm to 12 µm in length and 1.0 µm to 1.5 µm in width. The phase contrast between peri and para phase can be seen inverted at high amount of nanosilica (3% to 5% NS-MB) where para phase become increased. Para phase was classified as low stiffness while peri and catana phase were classified as high stiffness. Fig. (**6**) also shows that the addition of 3% to 5% NS did not give a significant influence towards the stiffness value of NS-MB.

3.3.2. Short-term Aged NS-MB

AFM images of asphalt binder after RTFO aged (short-term ageing) are shown in Figs. (**7** and **8**). Compared to unaged sample, the difference between the appearance of peri phase and para phase was obvious, where the para phase for RTFO aged NS-MB samples significantly disappear. Furthermore, the catana phase for all the specimens except 0% and 4% NS-MB also disappeared where there was only two distinctive phases could be identified, which were the image only displayed the bright spot and peri phase. This image indicates that the asphalt binder becomes stiffer after RTFO aged condition. This may be due to the chemical reaction occurrence and molecular structures changes of asphalt binder during ageing condition process. Catana and para phase could only be seen at high amount of nanosilica which was 4% and 5% NS-MB. The dimension of catana phase for both NS-MB became smaller compared to the unaged sample with average length and width approximately 3.5 µm to 4.5 µm and 0.8 µm to 1 µm respectively. In this condition, the highest catana phase was found at 3% NS-MB.

Fig (5). AFM Image (Unaged 0,1,2% NS-MB).

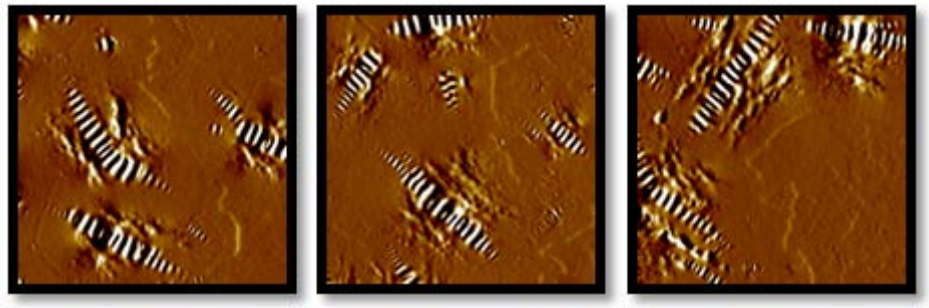

Fig (6). AFM Image (Unaged 3,4,5% NS-MB).

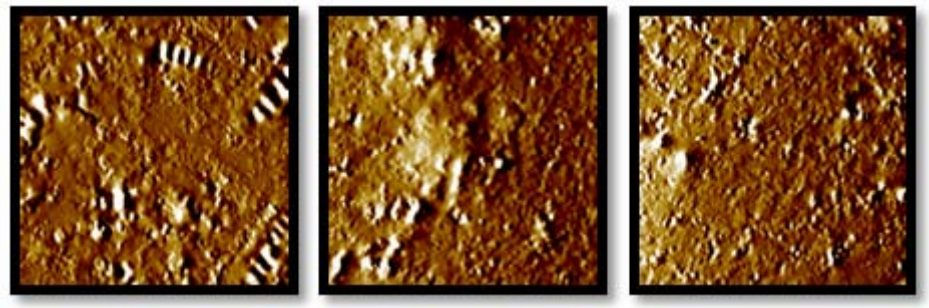

Fig (7). AFM Image (RTFO 0,1,2% NS-MB).

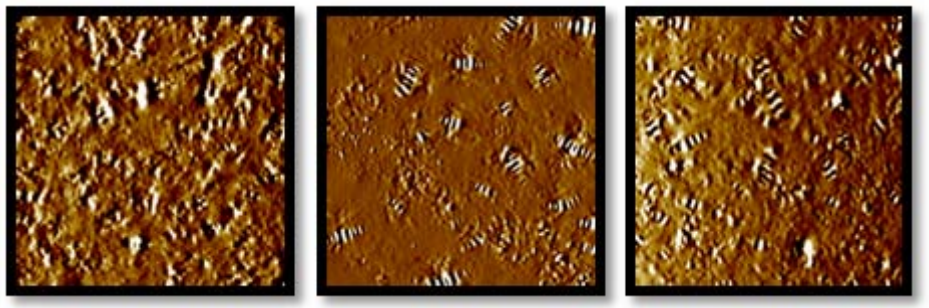

Fig (8). AFM Image (RTFO 3,4,5% NS-MB).

3.3.3. Long-term aged NS-MB

Figs. (**9** and **10**) show the AFM image of PAV aged (long-term aged) NS-MB samples. In this condition, all three phases were identified. The size of catana phase for 0% and 5% NS-MB were smaller compared to the remaining NS-MB specimens. The size of both specimens was approximately 2 µm to 3 µm in length and 500 nm to 600 nm in width, while the remaining specimens were about 7 µm in length and 1.25 µm in width. By comparing the unaged with aged images, the PAV aged images showed the highest distribution of catana phase. In addition, 2% NS-MB again shows the highest catana phase distribution and surface roughness. Thus, 2% NS-MB was determined as the stiffest specimen in terms of AFM evaluation.

Figs. (**11** and **12**) show the phase distribution and average roughness for all amounts of NS-MB and different ageing conditions. From the graph, it could be seen that the Peri phase for all three ageing conditions is higher compared to Catana phase and Para phase. Catana phase is increased with the addition of nanosilica from 10% to 15%. It shows that the addition of nanosilica enhanced the properties of asphalt binder. In terms of surface roughness, it is increased from 4.2% to 6.2% for unaged condition, 2.5% to 3.2% for short-term aged condition, and finally from 0% to 5% for long-term aged condition. It shows that nanosilica is capable of providing asphalt binder an adequate resistance towards ageing condition. The summary of the results is shown in Tables **3** and **4**. It exhibits that 2% and 3% nanosilica provide the best morphological performance for the asphalt binder. This finding

is similar to a study by Qin *et al*. (2014). For example, at unaged 2% NS-MB, Catana phase is increases from 10% to 15%, which is 50% increment. For short-term aged 3% NS-MB, Catana phase increases from 12% to 16%, which is about 33% increment. For long-term aged 2% NS-MB specimen, Catana phase is significantly increases from 14% to 22%, which is about 57% increment. It proved that the addition of NS is capable of providing the asphalt binder with sufficient resistance towards ageing effect.

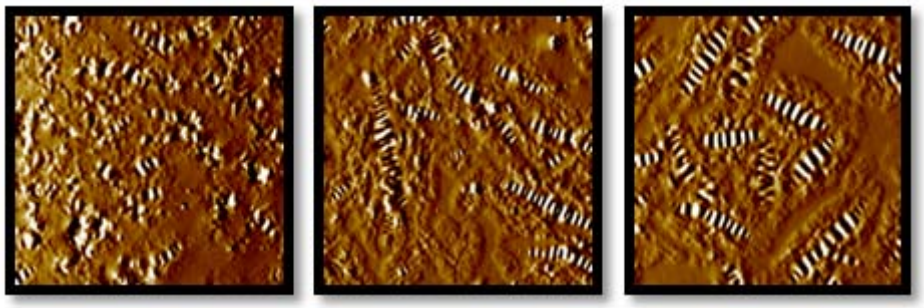

Fig (9). AFM Image (PAV 0,1,2% NS-MB).

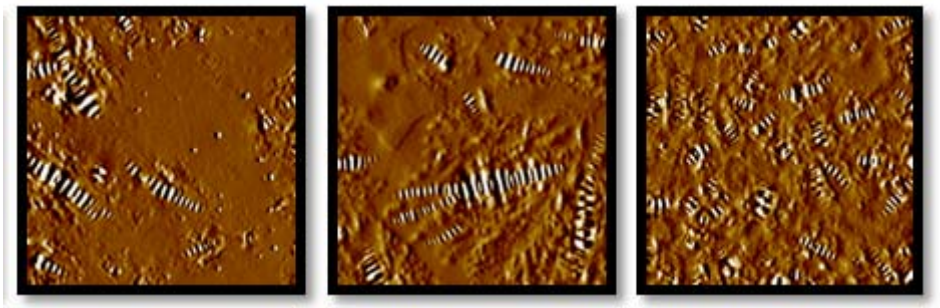

Fig (10). AFM Image (PAV 3,4,5% NS-MB).

Table 3. Phase distribution of modified binder.

Nanosilica Percentage (%)	Phase Distribution (%)								
	Unaged			RTFO aged			PAV aged		
	Catana phase	Peri phase	Para phase	Catana phase	Peri phase	Para phase	Catana phase	Peri phase	Para phase
0	10	65	25	12	85	3	14	82	4
1	13	58	29	5	95	0	21	72	7
2	15	65	20	8	92	0	22	66	12
3	8	29	63	16	84	0	13	61	26
4	10	33	57	9	80	11	12	71	17
5	10	40	50	10	90	0	14	85	1

Table 4. Average surface roughness.

Nanosilica Percentage (%)	Average Surface Roughness		
	Unaged	RTFO aged	PAV aged
0	4.191	2.505	0.004
1	4.457	3.204	4.069
2	6.249	3.246	5.062
3	4.342	2.712	2.631
4	5.039	2.152	4.227

(Table 4) cont.....

Nanosilica Percentage (%)	Average Surface Roughness			
	Unaged	RTFO aged	PAV aged	
5	5.736	0.002	3.164	
	Average	5.002	2.764	3.831

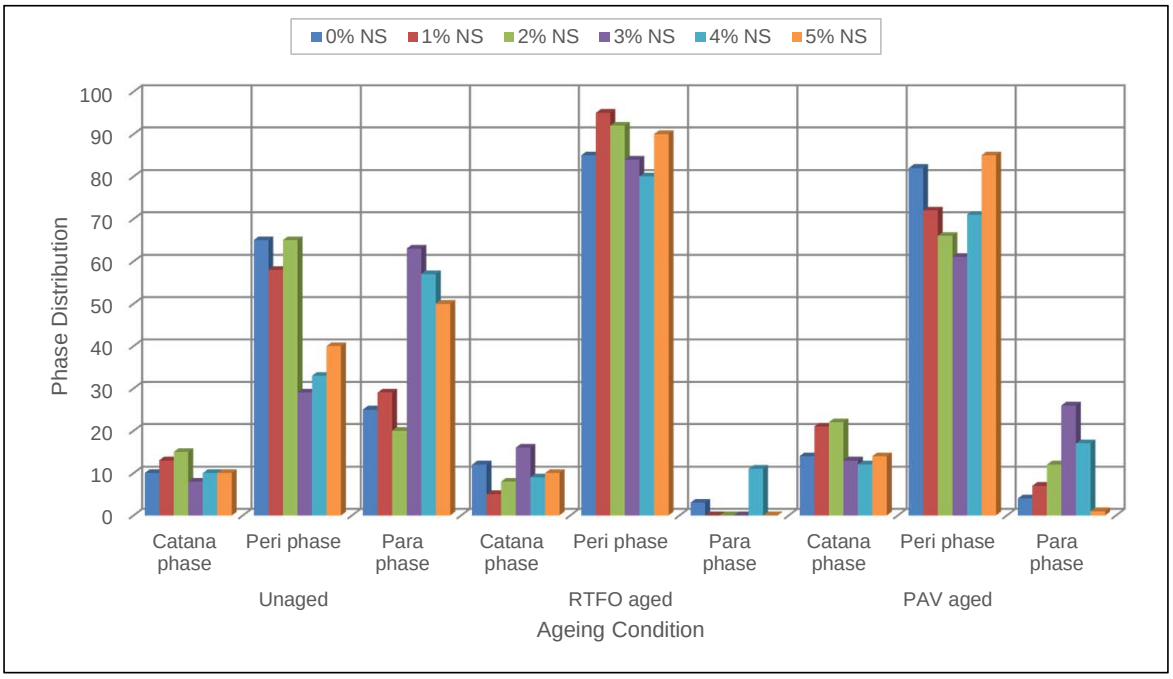

Fig (11). Phase Distribution.

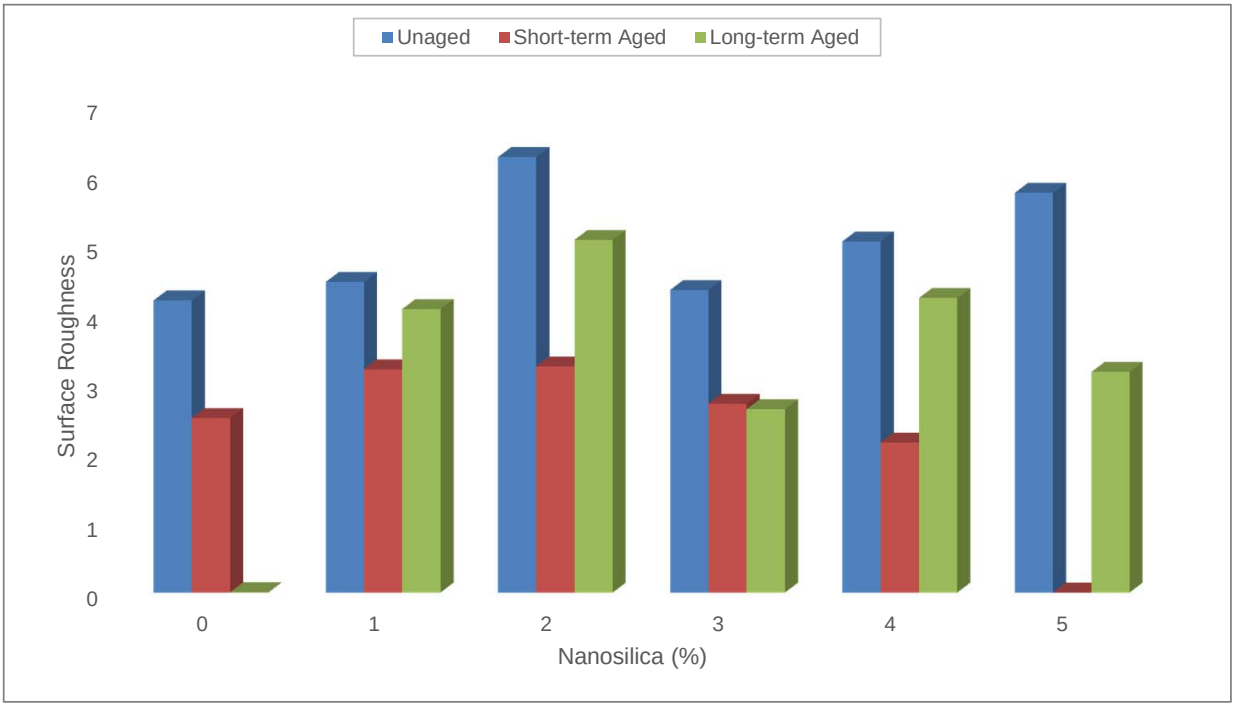

Fig (12). Surface Roughness.

3.4. Volumetric Properties of SMA

3.4.1. Stability

Fig. (**13**) shows the stability versus density values for SMA20 asphalt mixture with 0% to 5% NS. From the graph, maximum value of stability and density are obtained at 2% NS-MB. It was a clear trend for both parameters, where the stability and density increased to a maximum level at 2% NS-MB before decreasing. It is indicated that higher stability and density contribute to more resistance towards deformation. At 2% NS-MB, maximum stability reaches 2300 N with maximum density of 2.26 g/mm^3, compared to stability of 2000 N and density of 2.22 for 0% NS-MB. The increment is about 15% for stability and 2% for density. However, the addition of more than 2% NS did not increase both parameters respectively. There is a clear indication that the use of 2% NS in SMA mixture was more effective in enhancing stability and density Fig. (**14**) shows the values of stability *versus* flow. It could be seen that value of flow increased with the increment of NS. However, the increment is still within the limit based on Malaysian Public Work Department for Roadworks [23], where the flow should not be more than 4 mm.

3.4.2. Flow

The flow performance of asphalt mix at different percentages of NS is illustrated in Figs. (**15** and **16**). The modified SMA20 mixture produced inconsistent flow value when adding NS, where the flow values are in the range of approximately 2.3 mm to 4 mm. According to Malaysian Public Work Department Roadworks specification [23], the flow values for the purpose of surfacing and pavement under heavy traffic category should be in the range from 3 mm to 5 mm. Thus, all the specimens for this study passed the standard requirement.

3.4.3. Stiffness

Figs. (**17** and **18**) Illustrate the stiffness values of the SMA mixture with different amount of NS content. Theoretically, higher stiffness of asphalt mixture will give better resistance and durability. Flexible pavement surface distresses such as raveling and bleeding will decrease significantly for stiffer asphalt mixture. From the graphs, it shows that the addition of 2% NS provides the highest stiffness of SMA mixture. The value of stiffness at 2% NS is about 1350 N/mm, compared to only 1150 N/mm for control specimen. This indicates that the addition of NS improved the stiffness characteristic of asphalt mixture by 15%.

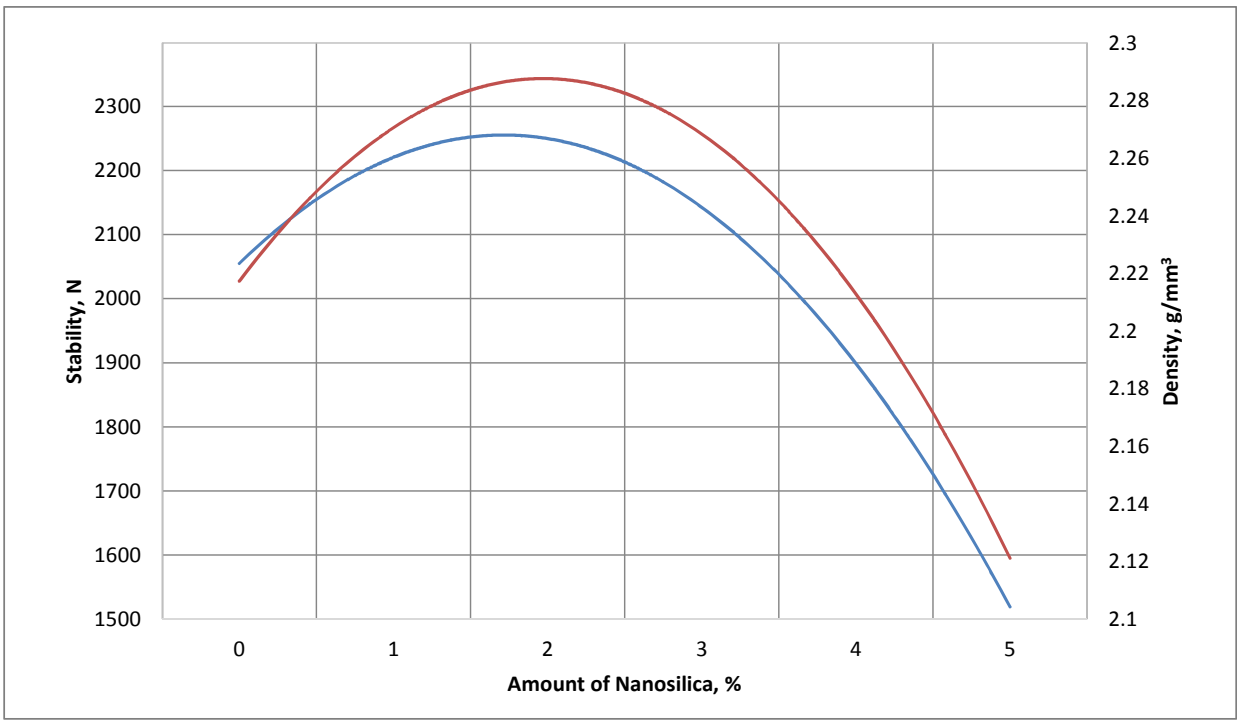

Fig (13). Stability and Density.

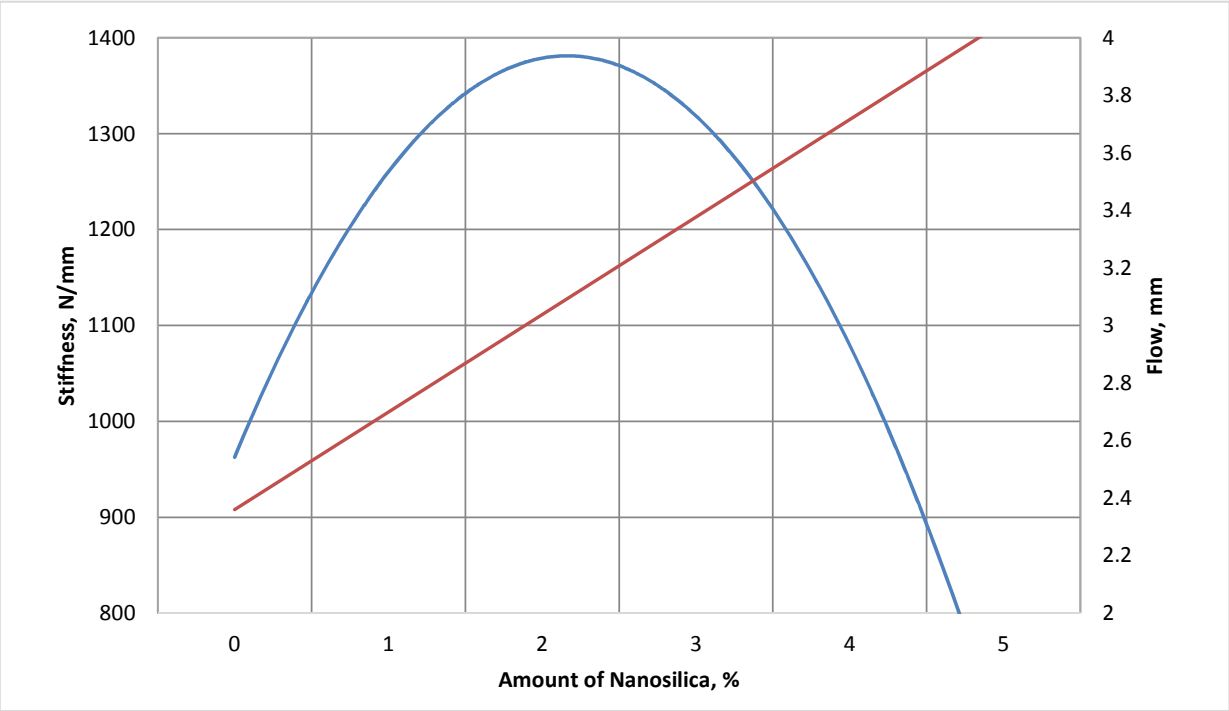

Fig (14). Stability and Flow.

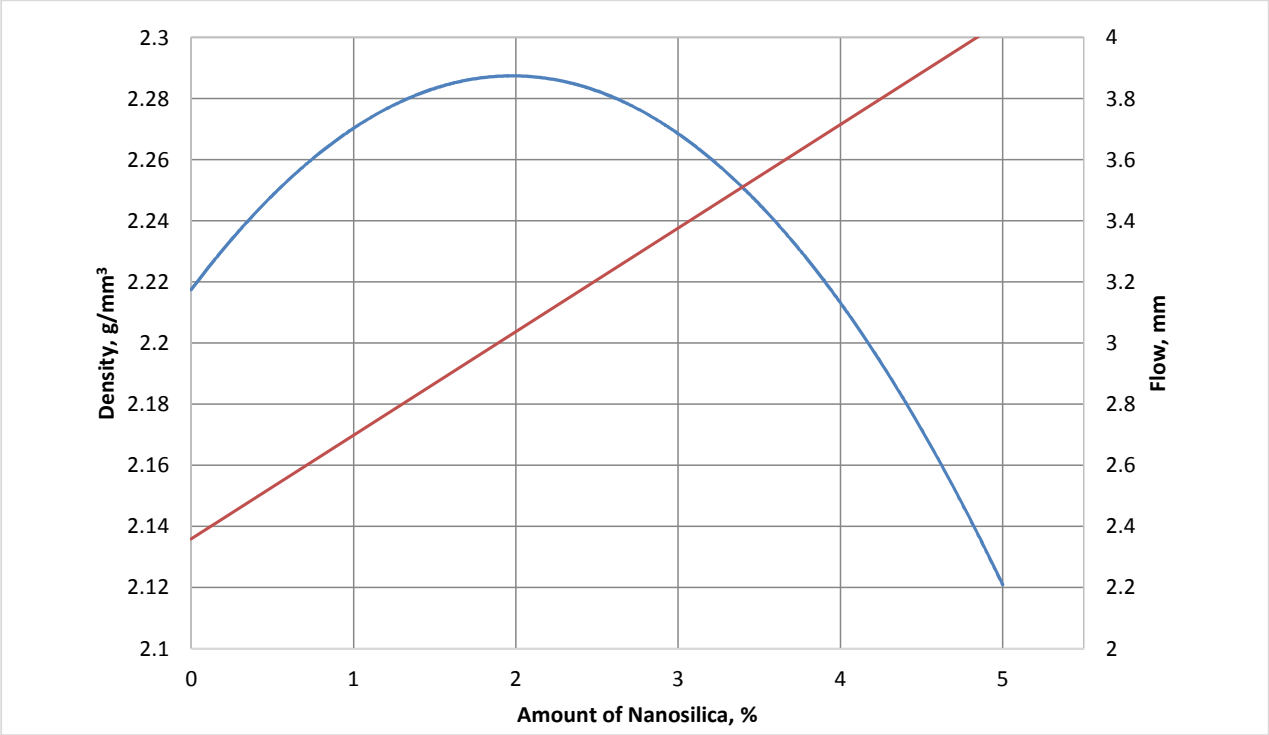

Fig (15). Density and Flow.

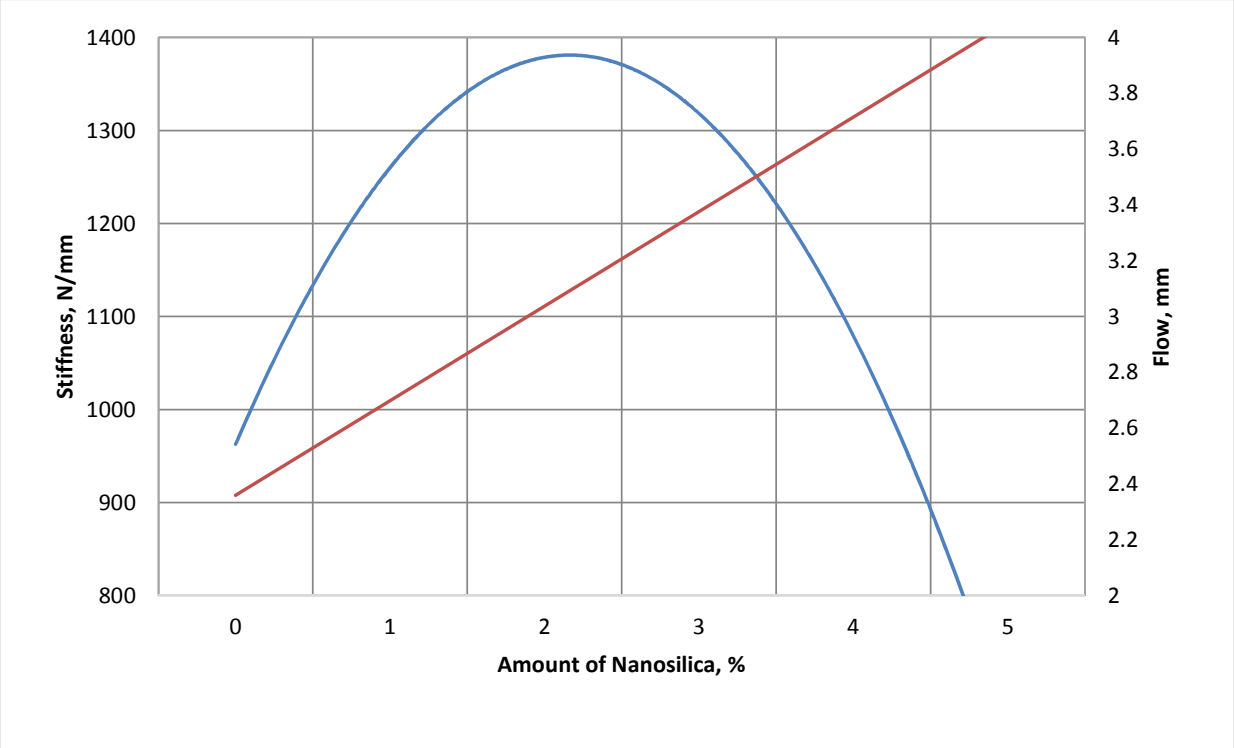

Fig (16). Stiffness and Flow.

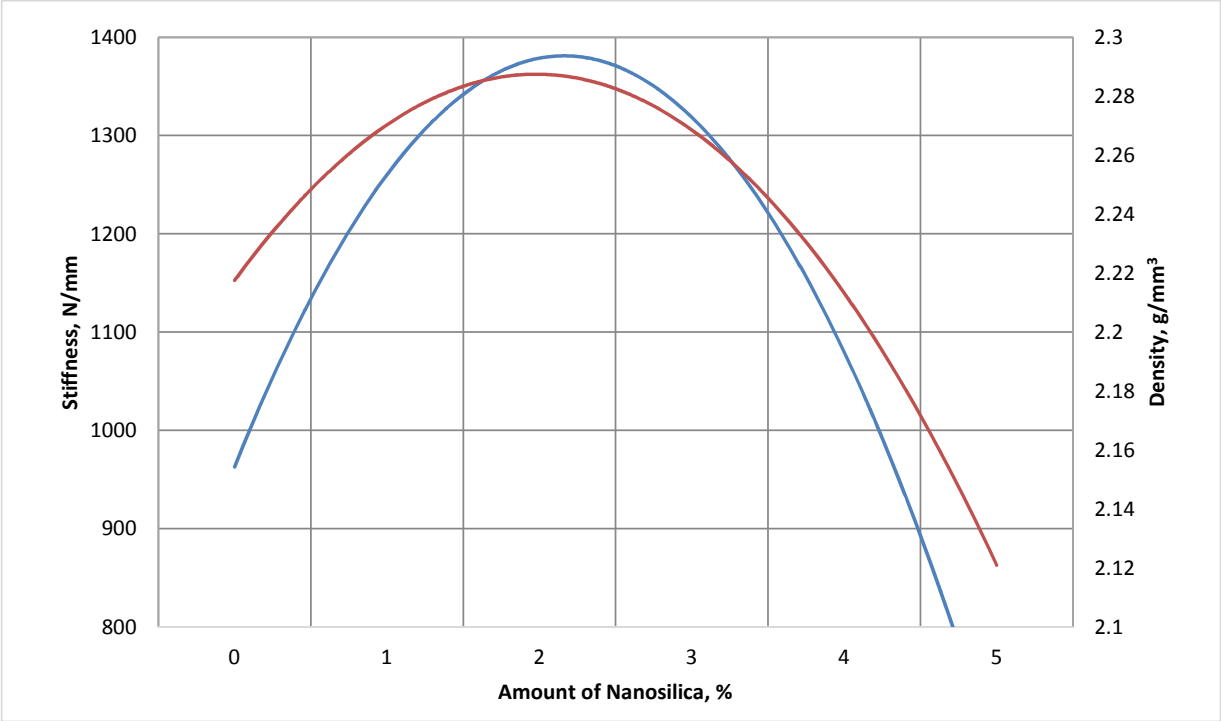

Fig (17). Stiffness and Density.

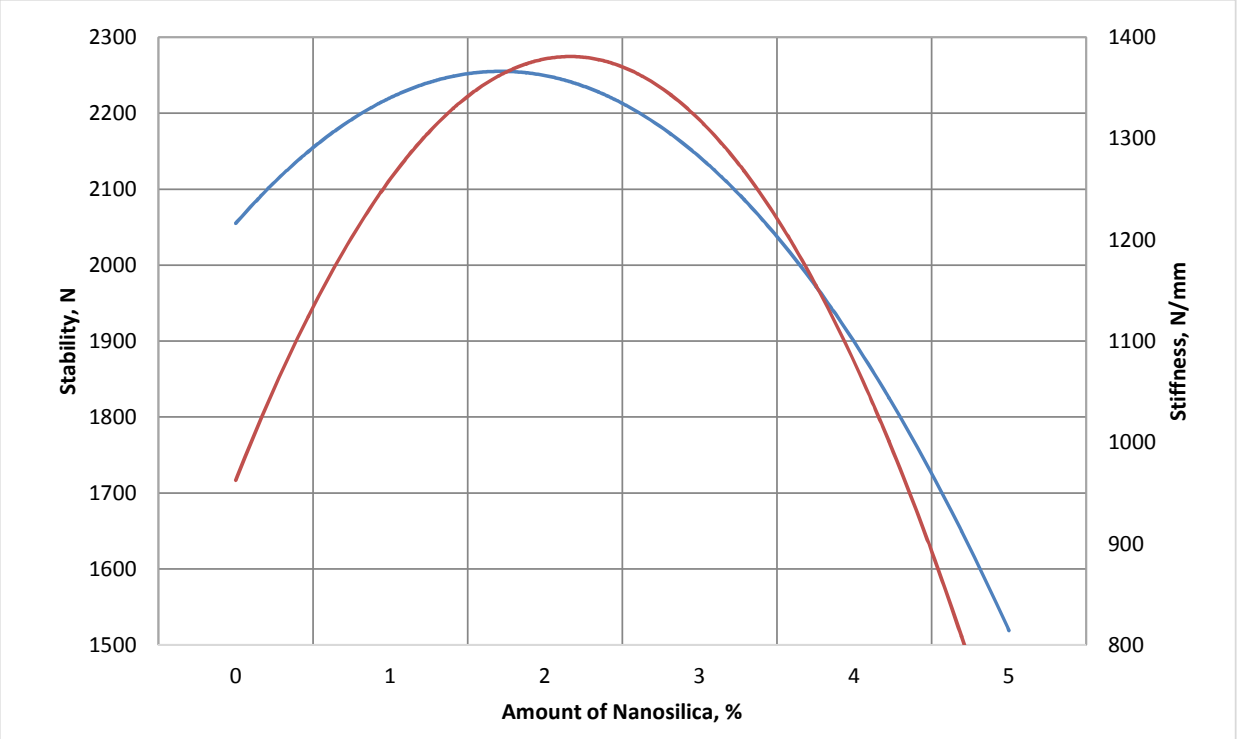

Fig (18). Stability and Stiffness.

CONCLUSIONS

From SEM image analysis and XRD evaluation, the existence of NS inside the asphalt binder was verified and proved that nanosilica can significantly improve the inner structure of asphalt binder. From AFM results, most of NS-MB images before and after ageing conditions displayed the typical bee structure (Catana Phase). The addition of NS in asphalt binder improved its surface stiffness. The overall surface stiffness of the asphalt binder after aging was increased and the surface became more solid. From the AFM image analysis also determined that 2% NS provides the stiffest value for asphalt binder. From volumetric properties evaluation for SMA, 2% NS-MB is also provides the highest values of stability and density. Thus, it can be concluded that the existence of nanosilica is capable of providing adequate resistance towards ageing effect for asphalt binder.

CONSENT FOR PUBLICATION

Not applicable.

AVAILABILITY OF DATA AND MATERIALS

The data supporting the findings of this article are available within this paper.

FUNDING

The authors would like to express deep gratitude to Universiti Malaysia Pahang and Ministry of Higher Education for funding this research under an internal grant with grant number RDU1803157 and FRGS-RACER Grant number RDU192604.

CONFLICT OF INTEREST

The authors declare no conflict of interest, financial or otherwise.

ACKNOWLEDGEMENTS

Declared none.

REFERENCES

[1] B. Singh, and P. Kumar, "Effect of polymer modification on the ageing properties of asphalt binders: Chemical and morphological investigation", *Constr. Build. Mater.,* vol. 205, pp. 633-641, 2019. [http://dx.doi.org/10.1016/j.conbuildmat.2019.02.050]

[2] A. Behnood, and M. Modiri, "Morphology, rheology, and physical properties of polymer-modified asphalt binders", *Eur. Polym. J.,* vol. 112, pp. 766-791, 2019. [http://dx.doi.org/10.1016/j.eurpolymj.2018.10.049]

[3] M. Enieb, and A. Diab, "Characteristics of asphalt binder and mixture containing nanosilica", *Int. J. Pavement Res. Technol.,* vol. 10, pp. 148-157, 2017. [http://dx.doi.org/10.1016/j.ijprt.2016.11.009]

[4] W. Ma, T. Huang, S. Guo, C. Yang, Y. Ding, and C. Hua, "Atomic force microscope study of the aging/rejuvenating effect on asphalt morphology and adhesion performance", *Constr. Build. Mater.,* vol. 205, pp. 642-655, 2019. [http://dx.doi.org/10.1016/j.conbuildmat.2019.01.151]

[5] D. Sun, B. Li, Y. Tian, T. Lu, X. Zhu, G. Sun, and F.A. Gilabert, "Aided regeneration system of aged asphalt binder based on microcapsule technology", *Constr. Build. Mater.,* vol. 201, pp. 571-579, 2019. [http://dx.doi.org/10.1016/j.conbuildmat.2018.12.167]

[6] A.K. Arshad, K.A. Masri, J. Ahmad, and M.S. Samsudin, "Investigation on Moisture Susceptibility and Rutting Resistance of Asphalt Mixtures Incorporating Nanosilica Modified Binder",

Pertanika J. Sci. Technol., vol. 25, pp. 19-30, 2017.

[7] L.M.B. Costa, H.M.R.D. Silva, J. Peralta, and J.R.M. Oliviera, "Using waste polymers as a reliable alternative for asphalt binder modification – Performance and morphological assessment", *Constr. Build. Mater.,* vol. 198, pp. 237-244, 2019.
[http://dx.doi.org/10.1016/j.conbuildmat.2018.11.279]

[8] B.B. Pizzorno, R.S. Antoun, E.D. Rodrigues, and L.F. Mathias, "Solvent effect on the morphology of the bee-structure observed by atomic force microscopy on bitumen sample", *Mater. Res.,* vol. 17, no. 5, pp. 1157-1161, 2014.
[http://dx.doi.org/10.1590/1516-1439.236113]

[9] T. Pauli, W. Grimes, A. Cookman, and S. Huang, "Adherence energy of asphalt thin films measured by force-displacement atomic force microscopy", *J. Mater. Civ. Eng.,* vol. 26, no. 12, pp. 1-11, 2014.
[http://dx.doi.org/10.1061/(ASCE)MT.1943-5533.0001003]

[10] R.G. Allen, D.N. Little, and A. Bhasin, "Structural characterization of micromechanical properties in asphalt using atomic force microscopy", *J. Mater. Civ. Eng.,* vol. 24, pp. 1317-1327, 2012.
[http://dx.doi.org/10.1061/(ASCE)MT.1943-5533.0000510]

[11] R. Jahangir, D. Little, and A. Bhasin, "Evolution of asphalt binder microstructure due to tensile loading determined using AFM and image analysis techniques", *Int. J. Pavement Eng.,* vol. 16, no. 4, pp. 337-349, 2014.
[http://dx.doi.org/10.1080/10298436.2014.942863]

[12] S.G. Jahromi, and A. Khodaii, "Effects of nanoclay on rheological properties of bitumen binder", *Constr. Build. Mater.,* vol. 23, no. 8, pp. 2894-2904, 2009.
[http://dx.doi.org/10.1016/j.conbuildmat.2009.02.027]

[13] J. Yang, and S. Tighe, "A review of advances of nanotechnology in asphalt mixtures", *Procedia – Soc. Behav. Sci.,* vol. 96, pp. 1269-1276, 2013.

[14] J. Xie, S. Wu, L. Pang, J. Lin, and Z. Zhu, "Influence of surface treated fly ash with coupling agent on asphalt mixture moisture damage", *Constr. Build. Mater.,* vol. 30, pp. 340-346, 2012.
[http://dx.doi.org/10.1016/j.conbuildmat.2011.11.022]

[15] A.B. Morgan, and J.W. Gilman, "Characterization of polymer-layered silicate (clay) nanocomposites by transmission electron microscopy and X-ray diffraction : A comparative study", *J. Appl. Polym. Sci.,* vol. 87, no. 8, pp. 1329-1338, 2002.
[http://dx.doi.org/10.1002/app.11884]

[16] K. A. Masri, A. K. Arshad, and M. S. Samsudin, "Samsudin, Mechanical properties of porous asphalt with nanosilica modified binder", *UTM. J. Teknol.,* vol. 78, no. 7-2, pp. 139-146, 2016.*Mechanical properties of porous asphalt with nanosilica modified binder.,* vol. 78, no. 7-2, pp. 139-146, 2016.

[17] A.B. Morgan, and J.W. Gilman, "Characterization of polymer-layered silicate (clay) nanocomposites by transmission electron microscopy and X-ray diffraction : A comparative study", *J. Appl. Polym. Sci.,* vol. 87, no. 8, pp. 1329-1338, 2002.
[http://dx.doi.org/10.1002/app.11884]

[18] H. Yao, Z. You, L. Li, C. H. Lee, D. Wingard, and Y. K. Yap, "Rheological properties and chemical bonding of asphalt modified with nanosilica", *J. Mater. Civ. Engineer,* vol. 25, no. 11, pp. 1943-5533, 2013.

[19] G. Liu, G. Leegwater, E. Nielsen, J. Komacka, and M.V.D. Ven, "Evaluating the rheological properties of PMB-containing RA binders from surface-layer asphalt mixtures to be recycled", *Constr. Build. Mater.,* vol. 49, pp. 8-14, 2013.
[http://dx.doi.org/10.1016/j.conbuildmat.2013.08.012]

[20] H. Yao, Q. Dai, J. Zhang, L. Sangtao, and X. Xiao, "Evaluation of contact angle between asphalt binders and aggregates using Molecular Dynamics (MD) method", *Constr. Build. Mater.,* vol. 212, pp. 727-736, 2019.
[http://dx.doi.org/10.1016/j.conbuildmat.2019.03.283]

[21] H. Yao, Z. You, L. Li, S.W. Goh, J. Mills-Beale, and X. Shi, "Evaluation of asphalt blended with low percentage of carbon micro-fiber and nanoclay", *J. Test. Eval.,* vol. 41, no. 2, pp. 278-288, 2013.
[http://dx.doi.org/10.1520/JTE20120068]

[22] H. Zhang, J. Yu, and S. Wu, "Effect of montmorillonite organic modification on ultraviolet aging properties of SBS modified bitumen", *Constr. Build. Mater.,* vol. 27, no. 1, pp. 553-559, 2012.
[http://dx.doi.org/10.1016/j.conbuildmat.2011.07.008]

[23]

[24] Q. Qin, M.J. Farrar, A.T. Pauli, and J.J. Adams, "Morphology, thermal analysis and rheology of Sasobit modified warm mix asphalt binders", *Fuel,* vol. 115, pp. 416-425, 2014.
[http://dx.doi.org/10.1016/j.fuel.2013.07.033]

[25] J. Xie, S. Wu, J. Lin, J. Cai, Z. Chen, and W. Wei, "Recycling of basic oxygen furnace slag in asphalt mixture: Material characterization & moisture damage investigation", *Constr. Build. Mater.,* vol. 36, pp. 467-474, 2012.
[http://dx.doi.org/10.1016/j.conbuildmat.2012.06.023]